Supplementary Figure 1 Hosokawa et al.

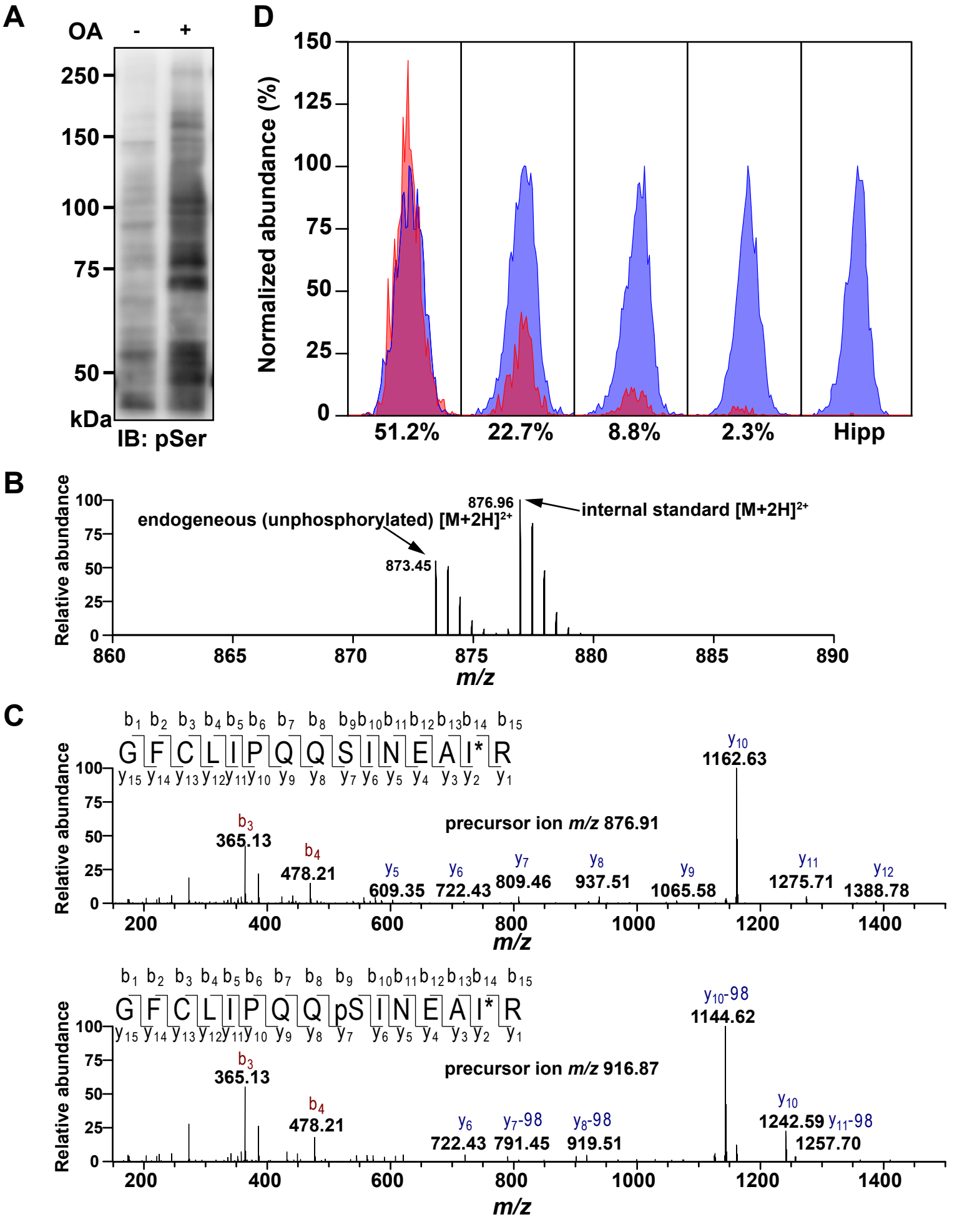

Supplementary Figure 2 Hosokawa et al.

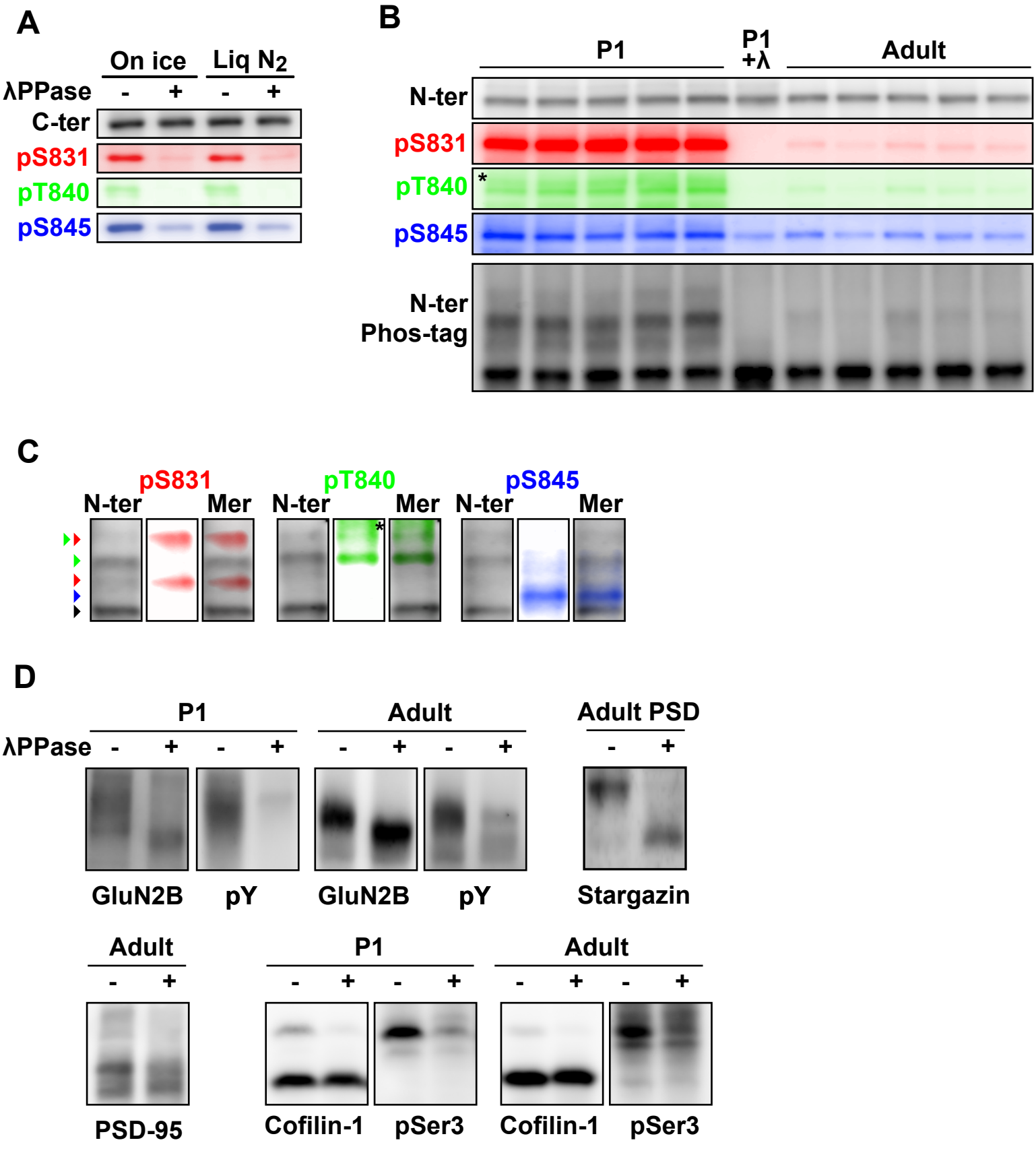

Supplementary Figure 3 Hosokawa et al.

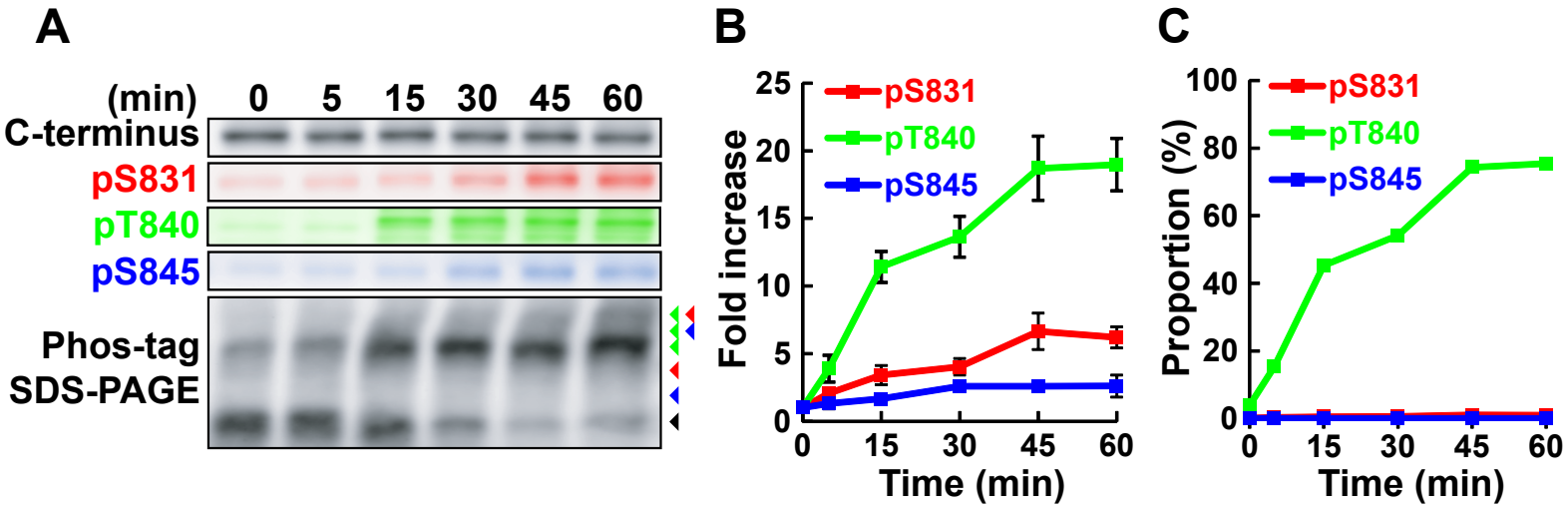

Supplementary Materials

Stoichiometry and phosphoisotypes of hippocampal AMPA type glutamate receptor phosphorylation

[1]Tomohisa Hosokawa, [2, 3]Dai Mitsushima, [1]Rina Kaneko and [1,4*]Yasunori Hayashi

1. Brain Science Institute, RIKEN, Wako, Saitama 351-0198, Japan.
2. Department of Physiology, Yokohama City University Graduate School of Medicine, Yokohama Kanagawa 236-0004, Japan
3. Department of Systems Neuroscience, Yamaguchi University Graduate School of Medicine, Ube, Yamaguchi 755-8505 Japan
4. Saitama University Brain Science Institute, Saitama University, Saitama 338-8570 Japan

Legends to Supplementary Figures

Supplementary Figure 1. Mass spectrometric quantification of phosphorylated GluA1 from HEK293T cells. Related to Figure 1.

(A) The treatment of HEK293T cells with okadaic acid increases phosphorylation of multiple proteins. The cells were treated with or without okadaic acid for 2 hours, homogenized, and separated on conventional SDS-PAGE. The sample was blotted with anti-phosphoserine antibody.

(B) Precursor ions corresponding to GluA1 [823] GFCLIPQQSINEAIR [837] from adult rat hippocampus. Those corresponding to chemically synthesized internal standard peptide were also detected.

(C) Product ion spectra for unphosphorylated (upper) / phosphorylated (lower) internal standards. I* indicates isoleucine labeled with ^{13}C and ^{15}N.

(D) Comparison of peak areas corresponding to S831 phosphorylated and unphosphorylated peptides from HEK293T homogenate containing GluA1 with different amount of S831 phosphorylation. The western blotting of the same samples separated on Phos-tag SDS-PAGE is shown in Fig. 1F. Peptides from GluA1 from adult hippocampus are also shown. The peaks represent the summation of four product ions, normalized by the abundance of internal standards. The peaks of the phosphorylated peptide were further normalized by the abundance

of unphosphorylated peptide for easy comparison.

Supplementary Figure 2. Expansion of phosphorylation analysis to GluA1 from various ages as well as to other postsynaptic proteins. Related to Figure 2.

(A) Confirmation that dephosphorylation does not take place during tissue dissection. Adult mouse forebrain was dissected on ice or rapidly frozen by liquid N_2 after sacrifice and homogenized by a Polytron homogenizer (Liq N_2). There was no significant difference in the tissue phosphorylation level between these two samples.

(B) Phosphorylation of GluA1 at P1 and adult hippocampus. Hippocampi from 5 animals from both ages were blotted with antibodies for GluA1 N-terminus, pS831, pT840, and pS845. The amount of GluA1 was preadjusted by performing a separate blot (not shown). The samples were separated by conventional (top 4 images) and Phos-tag (bottom image) SDS-PAGE. P1 sample treated with λ phosphatase is shown (P1+ λ). * here and in (C) indicate cross-reactivity to other proteins.

(C) Identification of GluA1 phosphoisotypes in P1 hippocampus. Bands corresponding to pS831, pT840, and pS831+pT840 can be identified but not to pS845 using the N-terminus antibody. Because we needed to load large amounts of protein due to low expression levels of GluA1 in P1 hippocampus, the band separation was not optimal. We therefore opted not to measure the precise proportion of phosphoisotypes.

(D) Detection of phosphorylation of various postsynaptic proteins. Hippocampal synaptosome was used except for Stargazin, for which PSD fraction was used. The separation of phosphorylated and unphosphorylated NR2B was not optimum due to the large size (180 kd) of this protein. The content of PSD-95 was low in P1 and was not analyzed here. Stargazin was not analyzed in P1 because PSD could not be purified from the P1 sample.

Supplementary Figure 3. Time course of the effect of phosphatase inhibition on GluA1 phosphorylation. Related to Figure 3.

Hippocampal dissociated neuronal culture were treated with okadaic acid and cyclosporine A and the time course of phosphorylation was monitored by antibodies against GluA1 C-terminal, pS831, pT840 and pS845 on conventional SDS-PAGE as well as with GluA1 C-terminal antibody on Phos-tag SDS-PAGE.

(A) Sample blot. Top four panels are conventional SDS-PAGE and bottom is Phos-tag SDS-PAGE. Expected positions of phosphoisotypes are shown in Phos-tag SDS-PAGE.

(B) Time course of phosphorylation after blockade of phosphorylation, expressed as fold change from the basal condition.

(C) Same as (B) but expressed as the proportion of the phosphorylated population to total amount. Data were calculated by multiplying the values in (B) by the proportion of phosphorylated GluA1 under basal condition in Fig. 3F. Error was not defined.

Supplementary Methods

Guidelines. All gene recombinant and animal experiments were in accordance with the institutional guidelines of the RIKEN, Yokohama City University, and Yamaguchi University.

Antibodies and reagents. Anti-GluA1 C-terminus (raised against 877-889), N-terminus, pS831, pS845, GluN2B, phosphotyrosine and stargazin antibodies were obtained from Millipore; anti-GluA1 pT840, and cofilin-1 from Abcam; anti-PSD-95 from Thermo Scientific; anti-cofilin-1 pS3 from Cell Signaling Technology; anti-synaptophysin from Sigma; okadaic acid and cyclosporine A from Wako; and protease inhibitor and phosphatase inhibitor cocktails from Nacalai Tesque.

Sample preparation from HEK293T cells. In order to induce phosphorylation in GluA1, we cotransfected HEK293T cells with a constitutively active T286D mutant CaMKII and further

treated the cells with 10 μM each of forskolin, phorbol 12-myristate 13-acetate, cyclosporine A and 1 μM okadaic acid. We later found that okadaic acid alone induces a similar pattern of phosphorylation. Therefore, we only used okadaic acid in some experiments. The cells were lysed in ice-cold RIPA buffer consisting of 10 mM Tris-HCl pH 7.5, 150 mM NaCl, 0.1% SDS, 1% NP-40, 0.5% sodium deoxycholate, protease inhibitor and phosphatase inhibitor cocktails and centrifuged at 10,000 g for 5 min to remove nuclei. We made a separate sample without phosphatase inhibitor for λ phosphatase treatment. The resultant supernatant was boiled after addition of Laemmli sample buffer and used for subsequent steps.

Subcellular fractionation of hippocampal tissue. Hippocampi were lysed in ice-cold RIPA buffer (as above) using a pestle homogenizer and centrifuged at 10,000 g for 5 min to remove nuclei. The resulting supernatant was used for western blotting after addition of Laemmli sample buffer. We made a separate sample without phosphatase inhibitor for λ phosphatase treatment.

The isolation of PSD fractions was performed as previously reported (Cho et al. 1992) but with modifications. Briefly, adult rat brain was homogenized by buffered sucrose (320 mM sucrose, 1 mM $NaHCO_3$, 1 mM $MgCl_2$, 0.5 mM $CaCl_2$). Homogenate was centrifuged at 1,400 *g* for 10 min and the supernatant was centrifuged at 13,800 *g* for 10 min to obtain a crude synaptosomal fraction. The pellet was resuspended in Triton buffer (10 mM Tris, pH 8.0, 0.5% Triton X-100, and phosphatase inhibitor cocktail), incubated for 1 hr and then centrifuged at 100,000 g for 1hr. The pellet was resuspended in Laemmli sample buffer and used as the PSD fraction. The supernatant obtained after centrifugation at 13,800 g was also ultracentrifuged at 100,000 g for 1 hr and the pellet was resuspended in Laemmli sample buffer and used as a high-density microsomal fraction. All procedures were performed at 0-4 °C.

To ensure that dephosphorylation does not occur during tissue dissection, the mouse skull was rapidly frozen in liquid N_2 after sacrifice. The forebrain was excised while the tissue was still

frozen and homogenized rapidly using a Polytron homogenizer. Then, the level of phosphorylation was compared with a sample dissected on ice. These two methods did not show any difference in the level of phosphorylated receptors (Fig. S2A). Therefore, for the rest of the study, we dissected the hippocampi on ice.

Quantification of phosphorylated GluA1 from blotting data. Quantification was performed in 16-bit blot images from LAS 3000 by Image J. A consecutive 1% incline of the moving average on the densitogramme of the C-terminus antibody blot was defined as the corresponding region of each phosphoisotype. The area of the region was calculated for the quantification of the proportion of each phosphoisotype.

AQUA of stoichiometry of GluA1 phosphorylation. Peptide synthesis and mass spectrometric analyses were carried out in the Research Resource Center at RIKEN Brain Science Institute. We first analyzed endogenous GluA1 from adult rat hippocampus with mass spectrometry and found that a peptide corresponding to the tryptic peptide containing S831 was readily detectable (Fig. S1B) whereas those containing T840 and S845 were not, possibly due to the peptide length or ionization efficiency. Therefore we focused on S831 phosphorylation. GluA1 was immunoprecipitated from transfected HEK293T cells or adult rat hippocampus in the presence of phosphatase and protease inhibitor cocktails similarly to Hayashi et al. (1997) and Nakagawa et al. (2005). The immunoprecipitate was separated on a conventional SDS-PAGE. The band was cut out after identification with Coomassie Brilliant Blue staining and digested with trypsin. As an internal standard for AQUA, chemically synthesized peptides corresponding to the tryptic peptide containing S831 with a phosphoserine (GF(carbamidomethyl C)LIPQQ(pS)INEAI*R) or without (GF(carbamidomethyl C)LIPQQSINEAI*R) were added to the sample. Isoleucine marked with * contained ^{13}C and ^{15}N so that we could distinguish the synthesized peptides from the corresponding

endogenous peptides by the difference of 7 Da. The digested samples were dissolved with 20 µl of 2% acetonitrile containing 0.1% formic acid. Five µl of each sample was injected into a separation column (75 µm x 150 mm, NANO-HPLC capillary column C18; Nikkyo Technos). The Easy-nLC 1000 Liquid Chromatography system (Thermo Fisher Scientific) was used for the peptide separation. The flow rate was set at 300 nl/min. The peptides were eluted with a gradient from 0 to 30% acetonitrile/0.1% formic acid and introduced into the mass spectrometer in-line. The Q-Exactive Hybrid Quadrupole-Orbitrap Mass Spectrometer and TSQ Vantage Triple Quadrupole Mass Spectrometer (Thermo Fisher Scientific) were used for peptide identification and quantification respectively. The spray voltage was set to 2300 V for both systems. Quantification of the amount of each peptide was performed with Thermo Scientific Pinpoint software. The peak areas of four product ions from the peptide containing S831 were summed and quantified (Kuhn et al. 2004).

Surface biotinylation and glycine-induced LTP. Surface biotinylation was carried out as described previously (Oh et al. 2006). Briefly, 14-16 DIV hippocampal neurons were treated with 1.0 mg/ml Sulfo-NHS-SS-biotin (Thermo Scientific) in extracellular fluid (125 mM NaCl, 2.5 mM KCl, 1 mM $MgCl_2$, 2 mM $CaCl_2$, 33 mM D-(+)-glucose, 25 mM HEPES) for 30 min on ice. The reaction was terminated by washing dishes with extracellular fluid containing Tris instead of HEPES. Cells were lysed with ice-cold RIPA buffer (as above) and subjected to avidin pull down. Glycine-induced LTP was performed in accordance with a previously reported protocol (Lu et al. 2001). Neurons were incubated in extracellular fluid containing 20 µM D-AP5 and 0.5 µM tetrodotoxin for 20 min followed by incubation in Mg-free extracellular fluid containing 3 µM strychnine, 20 µM bicuculline and 200 µM glycine for 10 min. Cells were further incubated in extracellular fluid for 30 min to allow time for AMPAR to traffic to synapses.

Inhibitory avoidance training. Experiments were performed as described previously (Mitsushima et al. 2011). Nine male Sprague-Dawley rats (postnatal 4-5 weeks of age) were used. Rats were housed on a constant 14-hour light/dark cycle (light on: 0500 - 1900) with *ad libitum* access to water and food. Before, 5 or 30 min after the training, the dorsal hippocampi were immediately dissected and processed to obtain the PSD fraction, which was subsequently subjected to Phos-tag SDS-PAGE.

Statistical analysis. All statistics were performed using an unpaired student's *t* test. $P < 0.05$ was considered statistically significant (see individual figure legends). Error bars represent SEM.

REFERENCES

Cho KO, Hunt CA, Kennedy MB. 1992. The rat brain postsynaptic density fraction contains a homolog of the Drosophila discs-large tumor suppressor protein. Neuron 9:929-42.

Hayashi Y, Ishida A, Katagiri H, Mishina M, Fujisawa H, Manabe T, Takahashi T. 1997. Calcium- and calmodulin-dependent phosphorylation of AMPA type glutamate receptor subunits by endogenous protein kinases in the post-synaptic density. Brain Res Mol Brain Res 46:338-42.

Kuhn E, Wu J, Karl J, Liao H, Zolg W, Guild B. 2004. Quantification of C-reactive protein in the serum of patients with rheumatoid arthritis using multiple reaction monitoring mass spectrometry and 13C-labeled peptide standards. Proteomics 4:1175-86.

Lu W, Man H, Ju W, Trimble WS, MacDonald JF, Wang YT. 2001. Activation of synaptic NMDA receptors induces membrane insertion of new AMPA receptors and LTP in cultured hippocampal neurons. Neuron 29:243-54.

Mitsushima D, Ishihara K, Sano A, Kessels HW, Takahashi T. 2011. Contextual learning requires synaptic AMPA receptor delivery in the hippocampus. Proc Natl Acad Sci U S A 108:12503-8.

Nakagawa T, Cheng Y, Ramm E, Sheng M, Walz T. 2005. Structure and different conformational states of native AMPA receptor complexes. Nature 433:545-9.

Oh MC, Derkach VA, Guire ES, Soderling TR. 2006. Extrasynaptic membrane trafficking regulated by GluR1 serine 845 phosphorylation primes AMPA receptors for long-term potentiation. J Biol Chem 281:752-8.